Available online at www.sciencedirect.com
SCIENCE DIRECT
ACADEMIC PRESS
Journal of Sound and Vibration 268 (2003) 809–824
JOURNAL OF SOUND AND VIBRATION
www.elsevier.com/locate/jsvi

Review

Aeroacoustics research in Europe: the CEAS-ASC report on 2002 highlights

E. Campos*

Instituto Nacional de Técnica Aeroespacial, Carretera a Ajalvir Km. 4, 28850 Torrejón de Ardoz, Madrid, Spain

Received 18 June 2003; accepted 2 July 2003

Abstract

This paper summarizes some highlights of aeroacoustics research in Europe in 2002, compiled from information provided to the Aeroacoustics Specialists Committee (ASC) of the Confederation of European Aerospace Societies (CEAS). The CEAS comprises the national Aerospace Societies of France (AAAF), Germany (DGLR), Italy (AIDAA), The Netherlands (NVvL), Spain (AIAE), Sweden (FTF), Switzerland (SVFW) and the United Kingdom (RAeS).

Contents

*Tel.: +34-91-520-1314; fax: +34-91-520-1939.
E-mail address: camposae@inta.es (E. Campos).

0022-460X/$ - see front matter
doi:10.1016/S0022-460X(03)00764-8

1. Introduction

The role of the Confederation of European Aerospace Societies Aeroacoustics Specialists Committee (CEAS-ASC) is to serve and support the scientific and industrial aeroacoustics community in Europe. Here "Aeroacoustics" is to encompass all aerospace acoustics and related areas. Each year the Committee highlights some of the research and development activities. This is the report of the 2002 highlights.

This paper consists of contributions made by the following people: S. Guidati, J.S.D. Ostertag, S. Wagner (University of Stuttgart), S. Lewy (ONERA, Chatillon), J. Fitzpatrick (Trinity College, Dublin), M. Billson, N. Andersson, L. Davidson, L.-E. Eriksson, (Chalmers University of Technology, Göteborg), C. Bailly (Ecole Centrale de Lyon), P. Jordan, Y. Gervais, J.-C. Valiere, (University of Poitiers), X. Zhang, X. X. Chen (University of Southampton), S.W. Rienstra, N.C. Ovenden (Eindhoven University of Technology), T. Elnady, H. Bodén (KTH, Stockholm), J. Yi (DLR Braunschweig), S. Hein, W. Koch (DLR Göttingen), T. Hohage (University of Göttingen).

2. Airframe noise

2.1. Phased microphone array measurements on an airfoil with flap

The German research project SWING (Simulation of Wing-Inflow Noise Generation) funded by Deutsche Forschungsgemeinschaft (DFG) deals with noise caused by high-lift devices of airplanes. The main mechanisms of flap side edge noise are investigated as part of a stepwise approach to the final problem which also includes trailing-edge noise of a profile, flap noise and wing tip noise. Experimental investigations had been performed in the laminar wind tunnel of the University of Stuttgart (LWK) and the acoustic wind tunnel of DLR Braunschweig (AWB). These acoustic measurements were carried out using an elliptic mirror and a phased microphone array (AAS).

Here, the focus is on AAS measurements of airframe noise originating from a two-dimensional (2D) airfoil with flap. Fig. 1 shows the sound pressure level (SPL) in dB measured at a wind speed of 60 m/s. The angle of attack of the configuration is 5°, the flap angle is 34°. The geometry is symbolized by solid black lines. The trailing edge of the main profile is obviously the dominant

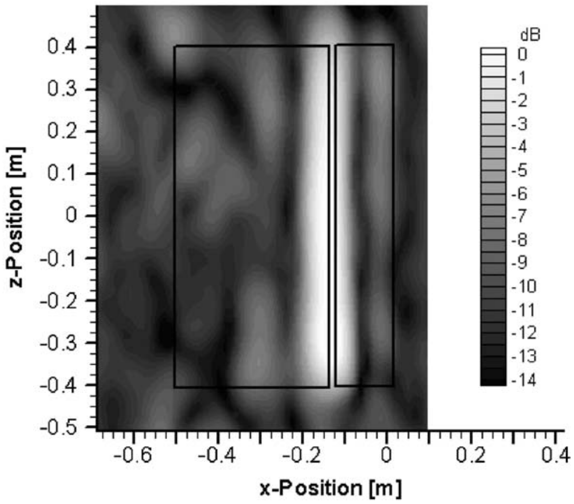

Fig. 1. Sound pressure level of the flap configuration. $U_\infty = 60\,\text{m/s}$, $\alpha_{total} = 5°$, $\alpha_{flap} = 34°$, $f = 4\,\text{kHz}$.

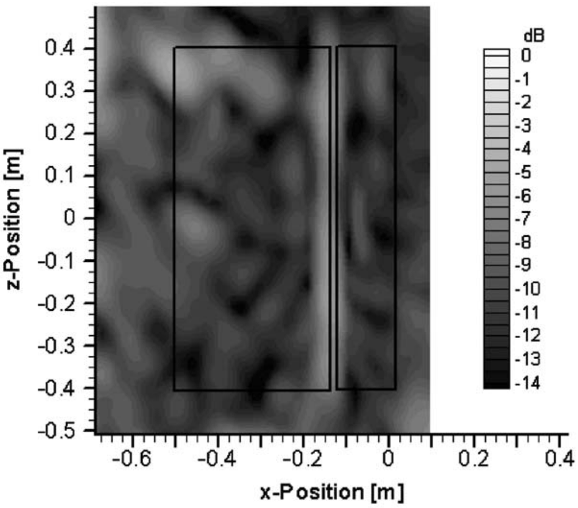

Fig. 2. Sound pressure level of the flap configuration with cove filling part. $U_\infty = 60\,\text{m/s}$, $\alpha_{total} = 5°$, $\alpha_{flap} = 34°$, $f = 4\,\text{kHz}$.

noise source. One explanation for the extremely high SPL is the detached flow in the cove. A filling part for the cove has been developed using flow visualization methods to maintain attached turbulent flow up to the trailing-edge of the main profile. Fig. 2 shows the SPL for this configuration. As expected the SPL at the trailing-edge is remarkably lower. The experimental data of all aerodynamic and acoustic measurements are used within the SWING project to validate the different numerical simulation tools which were developed by the project partners. (By Sandro Guidati, Jasmin S.D. Ostertag, Siegfried Wagner, *Institute of Aerodynamics and Gasdynamics*, *University of Stuttgart*, *Germany*.)

3. Fan and jet noise

3.1. Fan broadband noise

Prediction of ducted-fan broadband noise has become a challenge for controlling aircraft turbofan noise because that component dominates overall sound levels at subsonic rotation tip speeds. Activity has been pursued at ONERA during the past year. The model had first been established for a uniform flow inside the duct, the free medium being at rest (case of static tests) [1]. It is based on the Ffowcs Williams and Hawkings equation for a random rotating dipole, in which the freefield Green function is replaced by the Green function in a hard-walled cylindrical duct with uniform flow. Freefield directivity is deduced using the simple radiation model of Tyler and Sofrin. All the results presented in Ref. [1] neglected the flow velocity inside the duct to balance the in-duct and freefield sound powers. Indeed, sound powers are not equal if there is a flow mismatch on the duct exit.

Computations have been extended to a free medium in translation which better simulates flight conditions (the same velocity being taken in all the space). The model of Tyler and Sofrin is no longer valid, and a routine based on the full Kirchhoff integral equation has been implemented [2]. The code has been applied to tests run by Rolls-Royce in its Ansty noise compressor test facility (ANCTF) within the framework of the FANPAC European project. The main characteristics of the model fan are: diameter 0.864 m, 24 blades, hub-to-tip ratio 0.391, design rotation speed 10,100 r.p.m. The drag-to-thrust ratio is taken equal to 0.4. It has been first verified that all the previous results were well retrieved, both in the no-flow case and with flow only inside the duct. Fig. 3 shows that computations assuming a uniform flow in all the space now lead to the same acoustic power inside the duct (label "*Duct*") and in the free field ("*Free*"), for upstream ("*Upst*") as well as for downstream ("*Down*") radiation. This is a basic validation of the method. It is mainly found from comparison with the no-flow case ("$M = 0$") that flow velocity tends to increase rotor forward radiation, and to decrease aft radiation. It is also assessed that sound power, W, varies much more slowly than the conventional law in velocity, V, to the fifth power, but rather in $V^{2.25}$ (diagonal straight line in Fig. 3). This is in good agreement with measurements.

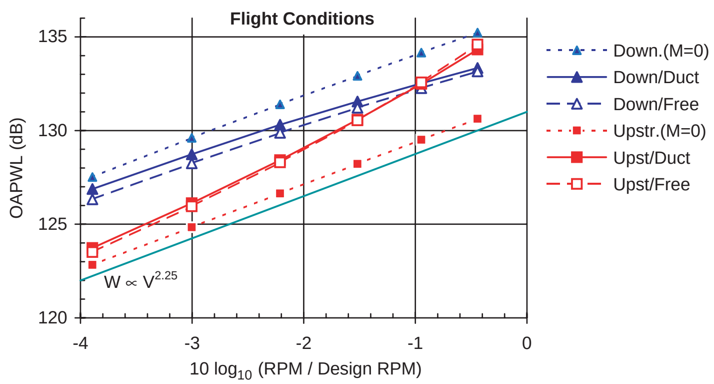

Fig. 3. Kirchhoff prediction of the overall sound power level, OAPWL, versus the logarithm of rotation speed, r.p.m.: Uniform flow in all the space.

It can be concluded that the computer code can already be used to estimate broadband sound levels radiated by a ducted fan, although some improvements are still planned. (By S. Lewy, *ONERA*, *Chatillon*, *France*.)

3.2. Jet exhaust aerodynamics and noise (JEAN) project

The JEAN project is funded under the 5th European Framework Program and has been running for nearly two years of a 3-year program. The objectives are to develop methodologies for the prediction of noise generated by jets including the effects of mixing enhancement and co-axial configurations. The long-term aim is to provide design tools for the development of low noise nozzles for HBR engines. The project is co-ordinated by the Mechanical Engineering Department at Trinity College, Dublin and there are 12 additional partners from the University, Research Establishment and Industry Sectors.

The work is fundamental and the project is divided into a management task and four work packages as follows:

- WP1—CFD prediction techniques.
- WP2—Acoustic source and propagation modelling.
- WP3—Experimental validation of CFD and acoustics.
- WP4—Application to advanced configurations.

For Work Package 1, a series of computations using the different CFD approaches have been performed for agreed configurations. A comparison of the CFD results from RANS methods was produced together with some preliminary results from the vortex technique. These showed that the RANS methods agreed quite well but the vortex method contained some discrepancies. For the LES method, the results show considerable progress in the capacity of this method to predict the evolutionary properties of jet flows and some results are given in Section 3.2.1. Direct noise computations (DNC) have been produced from the LES procedures as outlined in Section 3.2.2.

For Work Package 2, various noise source modelling methods have been investigated. For the acoustic analogy methods, the work has concentrated on adaptation of existing procedures to accommodate the output from the CFD codes. For the vortex source modelling, a method has been developed to utilize the output from the vortex based CFD models directly in the computation of acoustic source terms. The stochastic noise generation and radiation (SNGR) procedure has been used to implement source terms in the linearized Euler equations (LEE) which are then to be used to calculate the noise radiation in the far field. Radiation techniques based on Kirchhoff methods have also been developed, one based on a Helmholtz/Kirchhoff method and the other on a Kirchhoff/Ffwocs-Williams-Hawkings adaptation. Initial work has also been performed on the effect of the shear layer on propagation. Preliminary results from the SNGR and LEE approach are presented in Section 3.2.3.

For Work Package 3, the test matrix was fixed at an early stage of the project. Both hot and cold jets have been investigated for a range of operating conditions. A complete set of single point 2-component LDA measurements for four jet conditions has been obtained together with measurements of both near field and farfield acoustic data. Results from the aerodynamic measurements are outlined in Section 3.2.4. Multi point measurements using two LDA systems are planned for the next phase of the work.

Work Package 4 has not yet started but it is anticipated that the parameters for this will be discussed in the immediate future. (By J. Fitzpatrick, *Mechanical Engineering Department, Trinity College, Dublin, Ireland.*)

3.2.1. Large eddy simulation of a compressible nozzle/jet configuration

A large-eddy simulation (LES) of a compressible nozzle/jet configuration has been carried out, with the subsequent purpose of applying the results for jet noise prediction. A cold Mach 0.75 jet was simulated. The jet Reynolds number, based on the jet velocity at the nozzle exit plane and the nozzle diameter, was 50,000. The Favre filtered Navier–Stokes equations were solved, using a finite volume method with a low dissipative third order upwind scheme for the convective fluxes, a second order centered difference approach for the viscous fluxes, and a three stage second order Runge-Kutta time marching technique. A compressible form of Smagorinsky's sub-grid scale model was used for computation of the sub-grid scale stresses.

The calculations were performed using a block structured boundary fitted mesh with approximately 3,000,000 cells. Calculations have been performed on a parallel computer using a message passing interface (MPI). Absorbing boundary conditions based on characteristic variables were adopted for all free boundaries. Velocity components specified at the entrainment boundaries were obtained from corresponding Reynolds averaged Navier–Stokes (RANS) calculation. In order to diminish disturbances caused by the outlet boundary, a buffer layer was added at the domain outlet. The numerical results are in good agreement with the experimental data provided by Laboratoire d'Etudes Aerodynamiques de Poitiers, as shown in Fig. 4. This work has been reported in Ref. [3]. (By N. Andersson, L. Davidson, L.-E. Eriksson, *Department of Thermo and Fluid Dynamics, Chalmers University of Technology, Göteborg, Sweden.*)

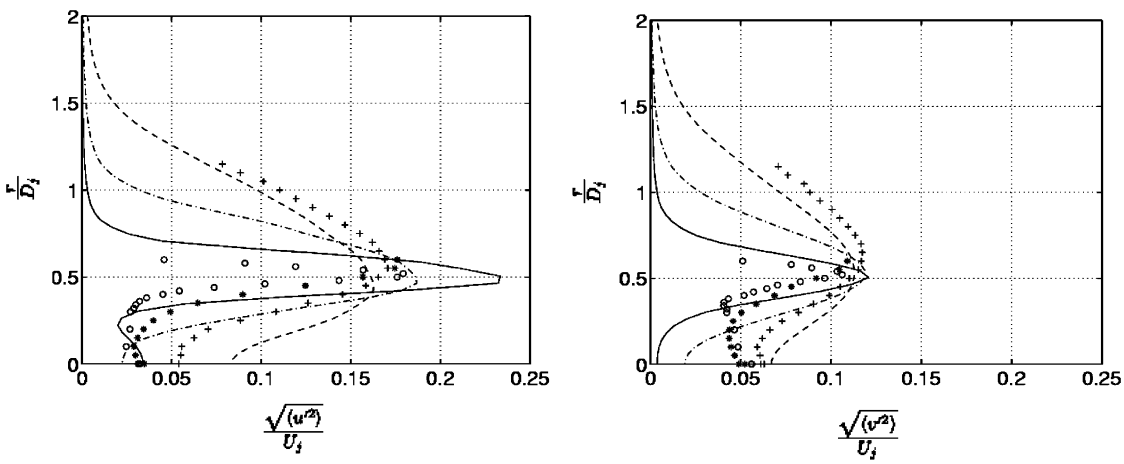

Fig. 4. Radial profiles of r.m.s. values of axial and radial velocity at three different axial positions are depicted in the left and right figure respectively. '○', '∗' and '+' correspond to experimental data at $x/D_j = 2.5$, 5.0 and 10.0. '-,' '–○' and '- -' represents LES data at the same axial positions.

3.2.2. Direct computation of aerodynamic noise

The investigation of jet noise mechanisms using direct noise computation (DNC) has been carried out [4]. DNC consists of computing the sound field radiated by turbulent flows from unsteady compressible simulations without acoustic modelling. The numerical solver combines highly accurate methods with spectral-like properties for the space-time discretization with effective non-reflecting boundary conditions. An $M = 0.9$ and $ReD = 4 \times 10^5$ circular jet has been studied by large eddy simulation (LES). The use of LES to compute aerodynamic noise is recent but of growing interest, since LES, unlike DNS, is not restricted to low Reynolds number flows. The flow and the sound field have been successfully compared with relevant measurements [5] and both correspond to what is expected for a high Reynolds number jet. A snapshot of the two fields is displayed in Fig. 5. Several critical points are discussed such as the subgrid-scale modelling which must preserve the effective Reynolds number of the flow. (A part of this work was supported by the EU research Programme JEAN, Jet Exhaust Aerodynamics and Noise, contract No. G4RD-CT-2000-00313.)

DNC using LES was also applied to study the noise radiated by full three-dimensional (3D) subsonic cavity flows [6]. The effects on self-sustained oscillations in the flow and on the radiated noise of parameters such as the thickness of the boundary layer, its laminar or turbulent state, or the spanwise width have been investigated. An illustration is shown in Fig. 6. (By C. Bailly, *Centre Acoustique LMFA*, *Ecole Centrale de Lyon*, *France*.)

3.2.3. Source terms for the linearized Euler equations

A formal derivation of the correct source terms for the linearized Euler equations on conservative form has been performed. Simplified versions of the derived source terms have also been developed. To validate the derived source terms a direct simulation of a forced 2D mixing

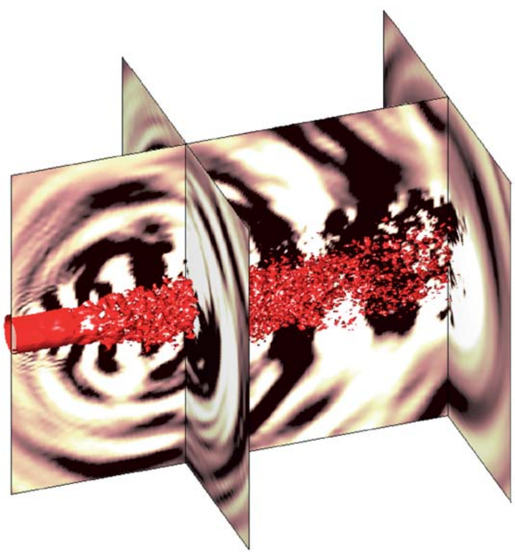

Fig. 5. Subsonic circular jet at $M = 0.9$ and $ReD = 4 \times 10^5$. 3D snapshot of the fluctuating pressure field outside the flow and of the norm of the vorticity field in the flow.

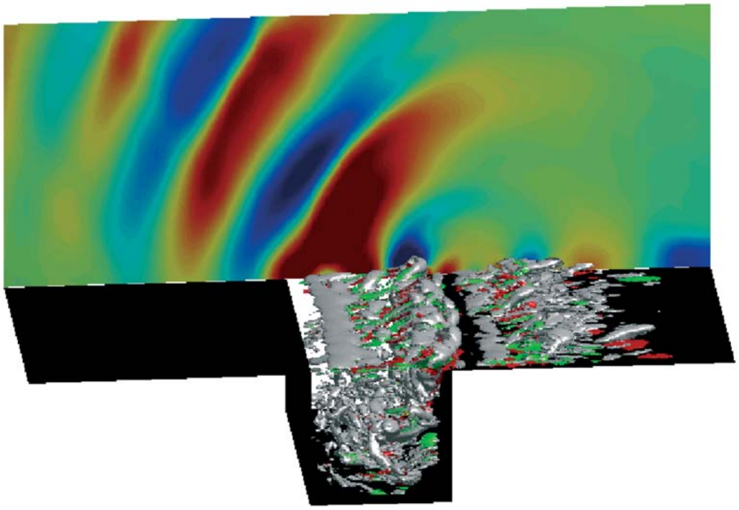

Fig. 6. Noise of a rectangular cavity with a laminar incoming boundary layer: $M = 0.6$, $ReD = 28700$, $L/D = 1$, $L/W = 0.5$ and $L = 2\,\text{mm}$. Snapshot of the fluctuating pressure field outside the cavity, and perspective view of the vorticity field (isosurfaces of Q-criterion).

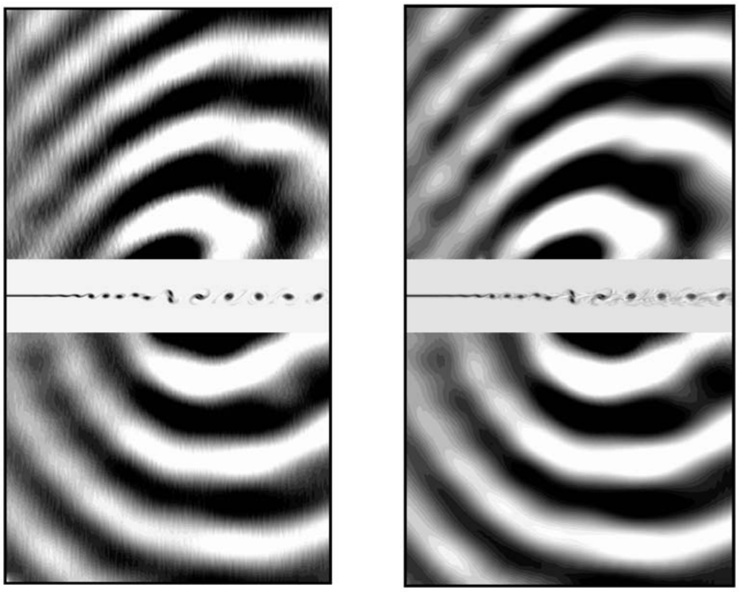

(a) (b)

Fig. 7. Vorticity and dilatation. (a) Direct simulation. (b) Linearized Euler simulation with full source terms.

layer has been carried out. The direct simulation has then been used to evaluate the derived source terms for the linearized Euler equations. The solution to the linearized Euler equations with the different versions of source terms were compared to the solution of the direct simulation and show good agreement which can be seen in Fig. 7.

This work, which is shown in Refs. [7,8], is part of an effort to further develop a method to predict jet noise called the stochastic noise generation and radiation (SNGR) method. This method uses the linearized Euler equations as an acoustic wave operator together with source terms, that are modelled. This is the first study in which a formal derivation of source terms for the linearized Euler equations on conservative form is performed. (By M. Billson, L.–E. Eriksson, L. Davidson, *Dept. of Thermo and Fluid Dynamics*, *Chalmers University of Technology*, *Göteborg, Sweden*.)

3.2.4. Jet aerodynamic measurements

Axial and radial jet velocities were measured simultaneously, using a two component LDV system operating in forward scatter. From these measurements, profiles of mean axial and radial velocities, turbulence intensities, and the (uv) component of the Reynolds stress tensor have been obtained at three axial positions for four jet conditions, with two of these at elevated temperatures. The four jets were compared at different axial positions and significant differences were observed between the hot and cold conditions. The isothermal jets were generally found to collapse onto one self-similar curve, while the hot jets collapsed onto another. This difference between hot and isothermal self-similar curves showed the dependence of spreading rate on jet temperature. Higher r.m.s. values of velocity in the hot jets at $x/D = 5$ were considered indicative of shorter potential cores.

Spectral measurements were obtained at 3 positions per profile, one on the jet axis, a second on the edge of the potential core (defined as that point where the mean velocity equals 95% of the exit velocity), and a third in the middle of the mixing layer. The spectral results for Jet 3 ($M = 0.75$, $T/T_a = 1$) are shown in Fig. 8. The Strouhal number was found to be a function both of the axial position of the measurement, and the temperature of the jet. For the isothermal jets (3 and 4) Strouhal numbers of 0.4, 0.6 and 1.1 were found to correspond to positions $x/D = 5$, $x/D = 2.5$ and $x/D = 1$, respectively, whereas for the hot jets these values are rather 0.3, 0.4 and 0.9. (By P. Jordan, Y. Gervais, J.-C. Valiere, *Laboratoire d'Etudes Aeródynamiques*, *University of Poitiers*, *France*.)

4. Duct acoustics

4.1. Sound propagation in and radiation from an exhaust duct

As part of the EU sponsored TurboNoiseCFD program, numerical methods have been developed to compute sound radiation from an exhaust duct. The numerical methods have several ingredients: in-duct propagation code based on multi-scale (MS) method of Eindhoven University of Technology (TUE), in-duct matching with University of Southampton high-order CAA code [9,10], near field sound propagation through solutions of linearized Euler equations and farfield radiation based on an integral surface representation (Ffowcs-Williams and Hawkings). In developing these methods, we have in mind sound radiation from either an intake duct or a bypass duct on an aero engine. In the case of radiation from either a bypass duct or a core nozzle, there are added issues associated with the presence of a shear layer between the exhaust flow and the external stream.

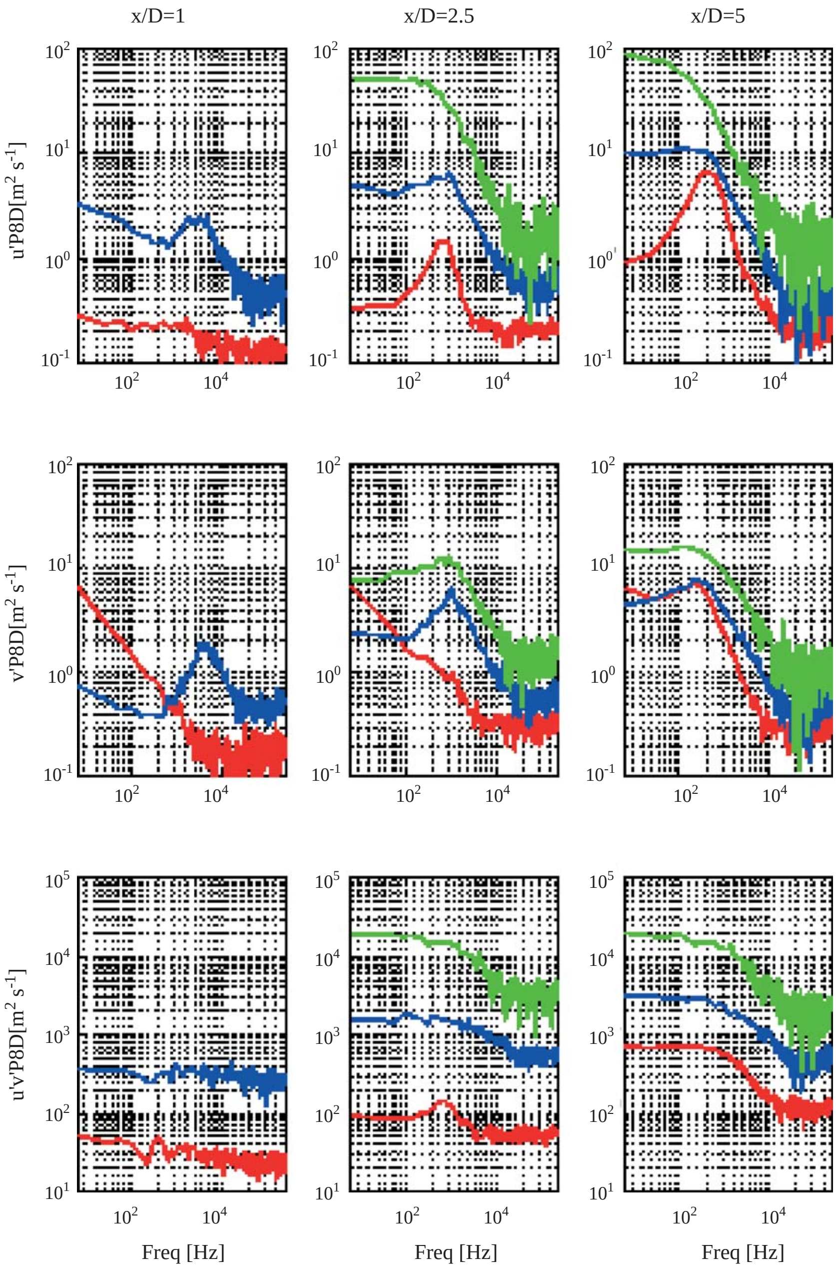

Fig. 8. Spectra for Jet 3 ($M = 0.75$, $T/T_a = 1$) (red—jet axis; blue—potential core edge; green—mixing layer center).

The numerical methods are used in a case study of sound radiation from a generic bypass duct; the study is conducted jointly between TUE and Southampton. The in-duct Mach number is 0.338. The exhaust stream is issued into a stationary environment. The incoming waves come from the TUE MS computation. A total of five radial modes exist. These form the inputs on the inflow boundary of the Southampton CAA computation and the target in an absorbing zone used to provide non-reflecting boundary conditions. The generic case study allows for a region near the exit plane of the bypass duct where predictions exist for both TUE and Southampton computations. This arrangement enables validation of the current methods. The in-duct wave pattern (Fig. 9(a)) shows a remarkable agreement between the TUE and Southampton predictions, up until very near the exit plane. This gives confidence to both methods. The fact that the MS code can be used close to the exit plane also suggests an efficient way to compute sound radiation from an exhaust duct; the matching between the duct propagation code and the propagation code can now be made close to the exit plane.

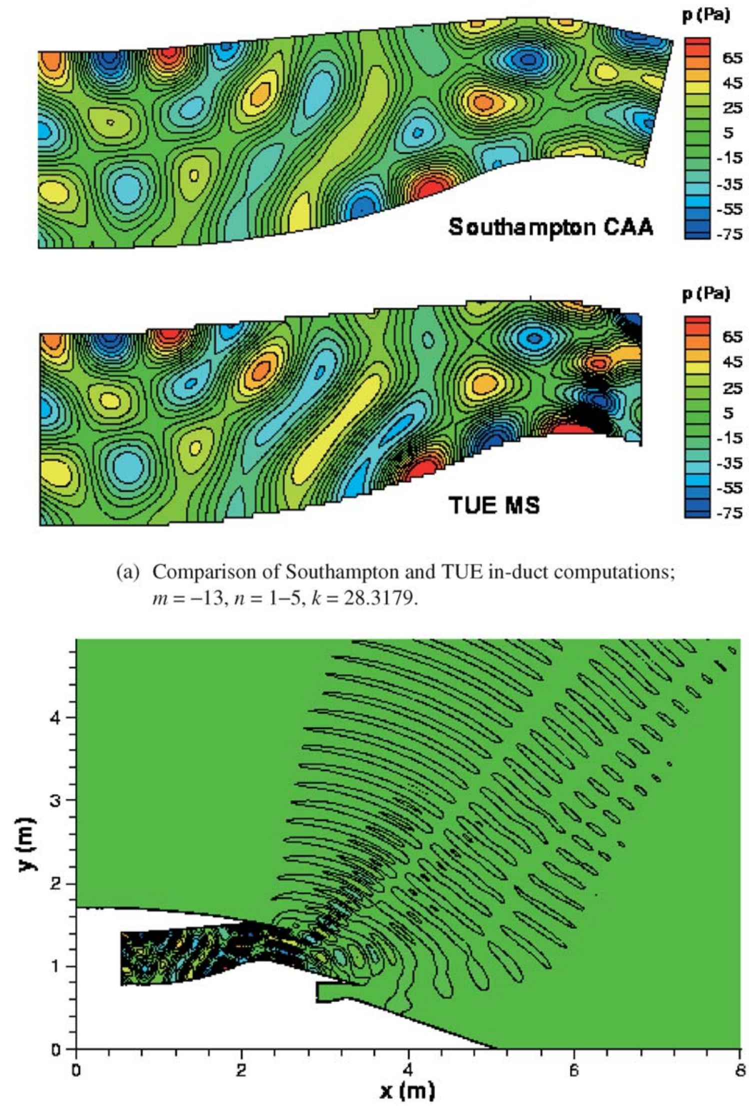

(a) Comparison of Southampton and TUE in-duct computations; $m = -13$, $n = 1$–5, $k = 28.3179$.

(b) Near field propagation.

Fig. 9. Sound propagation in and radiation from a generic bypass duct.

The near field wave pattern is given in Fig. 9(b). The overall directivity pattern in the far field is dominated by the $n = 1$ radial mode below $\theta = 50.3^{\circ}$ which is the angle of the main radiation peak for the $n = 1$ mode. However, the overall directivity has a main radiation peak at 62.4° which is not dominated by any of the radial modes. Rather it is a combination of all the radial modes. It is interesting to observe that the overall farfield directivity does not reveal sharp interference dip angles as observed in the earlier exhaust duct computations where the shear layer is modelled as a vortex sheet. There is a broadening of the directivity content over the observation angle range. (By X. Zhang and X.X. Chen, *University of Southampton*, *UK*, *and* N.C. Ovenden and S.W. Rienstra, *Eindhoven University of Technology*, *The Netherlands*.)

4.2. Near cut-on cut-off transition in lined ducts

It is a well-known fact that an isolated cut-on acoustic mode can be made to undergo a complete reflection in a hard-walled duct with varying cross-section. A multiple-scales analysis of these turning points, as performed in Refs. [11,12], reveals that conservation of energy considerations in an irrotational mean flow require complete reflection of the mode, as the resulting cut-off mode carries no energy.

Recent work on applying multiple-scales methods to acoustic propagation at Eindhoven University of Technology (for the EC project TurboNoiseCFD) has led to the discovery that similar turning-point phenomena can occur even in lined ducts. The analysis presented in Ref. [13] demonstrates that for an attenuated mode which undergoes the so-called near transition (in an irrotational mean flow), the energy lost by the mode is often significantly greater than the energy absorbed by the impedance wall. A partial reflection of the original mode is shown to provide the explanation for this discrepancy. The magnitude and phase of the reflection coefficient are determined as a function of the wall impedance and remain consistent with previous analyses in the hard-wall limit. (By N.C. Ovenden, *Eindhoven University of Technology*, *The Netherlands*.)

4.3. Hard strips in lined ducts

Acoustic liners are widely used to attenuate sound waves inside aircraft jet engines. In most cases, the existence of hard strips in the lined ducts is inevitable. Previous research has proved that segmenting the liner and the positioning of the liner segments affect the attenuation characteristics of the liner. The aim of this work is to investigate these effects, and to compare the properties of circumferentially segmented duct liners with those of uniform liners, in order to identify any potential benefits of circumferentially segmented liners. The point-matching method is used to analyze the problem. It is a straightforward numerical method based on a closed form ansatz, which fulfils the governing equations and is matched to the boundary conditions point-wise. A computer code is used to obtain the wave numbers of the different modes, from which the transmission loss for each mode can be calculated at the desired range of frequencies. The present study [14] included both locally reacting and non-locally reacting liners. It was found that non-locally reacting liners are better acoustic attenuators and are less affected by the presence of hard strips than locally reacting liners, where the behavior of each mode depends on the number and width of hard splices in the duct (Fig. 10). (By T. Elnady and H. Bodén, *Marcus Wallenberg Laboratory for Sound and Vibration Research*, *KTH, Stockholm*, *Sweden*.)

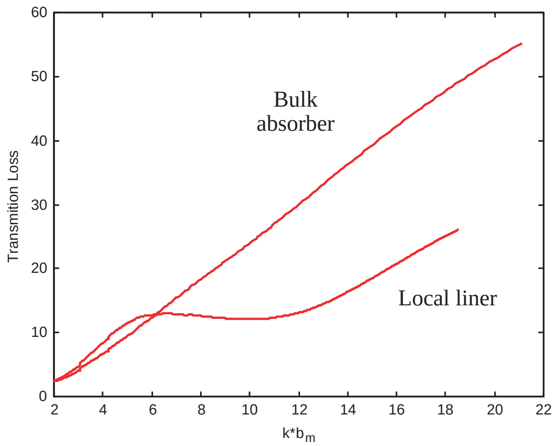

Fig. 10. Comparison between the total transmission loss for a duct with no splices lined with either a bulk absorber or a locally reacting liner.

5. Helicopter noise

5.1. Tail rotor noise under main/tail rotor interaction

To demonstrate the effects of main rotor (MR) and tail rotor (TR) mutual interaction on the aerodynamics and noise characteristics, a BO105 MR/TR configuration is chosen in the numerical simulations. A *MA*i*N* and *T*ail rotor *I*nteraction *C*ode based on *U*nsteady free wake 3D *P*anel *M*ethod, (UPM-MANTIC) [15] is used to account for the mutual aerodynamic interference between MR and TR. The unsteady pressure on the MR and TR blade surface is calculated with UPM-MANTIC and used as input to another DLR aeroacoustic code, *A*eroacoustic *P*rediction *S*ystem based on *I*ntegral *M*ethod (APSIM) [16], to calculate rotor noise.

Free wake and rotor noise computations were performed to study the effect of MR/TR mutual interaction on rotor wake development, blade loads and noise radiation [17]. With the special emphasis on tail rotor noise, a climb flight is simulated. Fig. 11 shows how the main and tail rotor interact in the development of the rotor wakes in 12° climb flight condition. The strong merging of the MR and TR wakes is demonstrated. The MR blades are seen to come clear of their wakes as these are, during the climb mode, pushed down and away from the MR disc. The edges of the MR wake show the tendency to be rolled-up. The TR blades cut through the MR wake. The MR blade passes close to the edge of the TR wake but does not intersect it. Fig. 12 shows the effect of MR/TR interaction on the TR noise. The single hot spot visible for isolated TR in Fig. 12(a) is replaced by two hot spots on either side of the TR disc for the MR/TR interaction case, Fig. 12(b). The position of the TR is represented by a straight line in the plots. An increase of the noise level on both sides of the TR disc due to MR/TR interaction is observed. (By J. Yin, *Institute of Aerodynamics and Flow Technology*, *DLR Braunschweig*, *Germany*.)

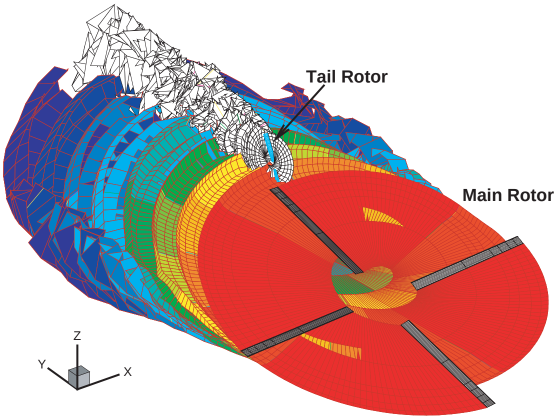

Fig. 11. Perspective view of MR and TR wakes.

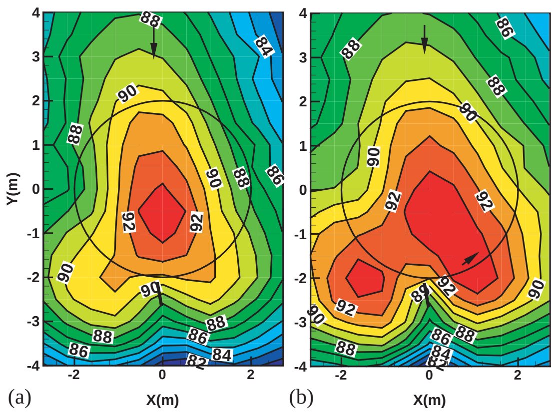

Fig. 12. Mid-frequency noise contours for TR. (a) Isolated TR, (b) TR under MR/TR.

6. Techniques and methods in aeroacoustics

6.1. Numerical computation of acoustic resonances in open systems

Resonances are extremely useful in a variety of wave propagation problems, e.g., lasers or musical instruments. In other applications they are detrimental and cause high loads or noise levels. Resonances in open systems are difficult to compute numerically due to reflections at the necessarily finite grid boundaries. This can be remedied by means of perfectly matched layer (PML) absorbing boundary conditions as introduced by Berenger [18].

Applying such absorbing boundary conditions to the Parker mode problem [19,20], a model problem for shear-layer excited resonances, yields not only the trapped (undamped) Parker modes, but also higher-order leaky modes, cf. Fig. 13 for an aspect ratio $l/d = 1.8$. Here l is the plate length, d the plate spacing and $f^* = kd/\pi$ denotes the dimensionless frequency. In addition to the discrete approximation of the continuous spectrum, corresponding to the cut-on modes,

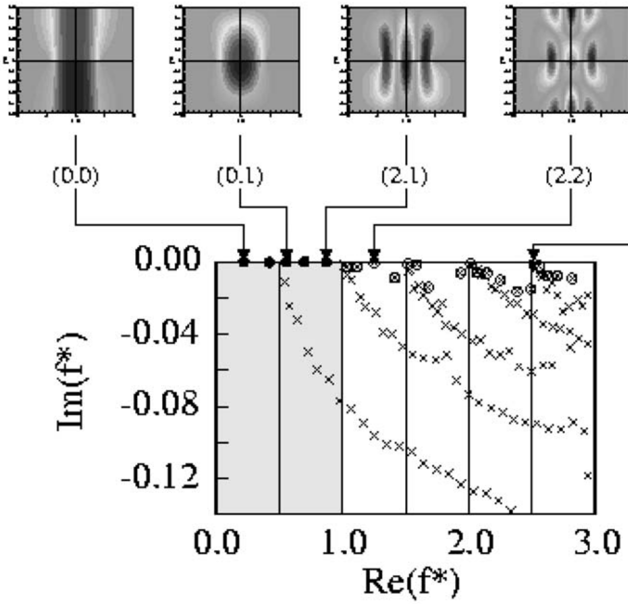

Fig. 13. Spectrum of trapped and leaky Parker modes with samples of corresponding eigenfunctions.

resonant modes occur which are marked by circles. The solid circles correspond to the few trapped modes. The modes with small imaginary part, corresponding to low damping, are expected to be of prime physical importance. Examples of relevant eigenfunctions are also depicted in Fig. 13. The ultimate goal of this work is to compute the resonances of high-lift devices, where such resonances are apparently causing high-level peaks in the radiated airframe noise. (By S. Hein and W. Koch, *Institute of Aerodynamics and Flow Technology*, *DLR Göttingen*, and T. Hohage, *Institute of Numerical and Applied Mathematics*, *University of Göttingen*, *Germany*.)

Acknowledgements

The compilation of the CEAS-ASC report on 2002 Highlights was supported by the X2-NOISE External Aircraft Noise Thematic Network, funded by the European Commission.

References

[1] S. Lewy, Computation of broadband noise radiated by a ducted fan, *International Journal of Acoustics and Vibration* 7 (3) (2002) 141–153.
[2] S. Lewy, Computation of broadband noise radiated by a ducted fan in an uniform flow, *10th International Congress on Sound and Vibration*, Stockholm, Sweden, 7–10 July 2003.
[3] N. Andersson, L.-E. Eriksson, L. Davidson, Large-eddy simulation of a Mach 0.75 jet, *9th AIAA/CEAS Aeroacoustics Conference*, Hilton Head, SC, 12–14 May 2003 (Paper submitted).

[4] C. Bogey, C. Bailly, D. Juvé, Noise investigation of a high subsonic, moderate Reynolds number jet using a compressible LES, *Theoretical and Computational Fluid Dynamics* 16 (4) (2003) 273–297.
[5] C. Bogey, C. Bailly, Direct computation of the sound of a high Reynolds number subsonic jet, *CEAS Workshop From CFD to CAA*, Athens, Greece, 7–8 November 2002 (see also *9th AIAA/CEAS Aeroacoustics Conference*, AIAA Paper 2003-3170 and *16th AIAA Computational Fluid Dynamics Conference*, AIAA Paper 2003-3557).
[6] X. Gloerfelt, C. Bogey, C. Bailly, D. Juvé, Aerodynamic noise induced by laminar and turbulent boundary layers over rectangular cavities, *8th AIAA/CEAS Aeroacoustics Conference*, Breckenridge, CO, 17–19 June 2002, AIAA Paper 2002-2476 (see also *CEAS Workshop From CFD to CAA*, Athens, Greece, 2002).
[7] M. Billson, Computational Techniques for Jet Noise Predictions, Lic. Thesis, Department of Thermo and Fluid Dynamics, Chalmers University of Technology, Göteborg, 2002.
[8] M. Billson, L.–E. Eriksson, L. Davidson, Acoustic source terms for the linear Euler equations in conservative form, *8th AIAA/CEAS Aeroacoustics Conference*, Breckenridge, CO, 17–19 June 2002, AIAA Paper 2002-2582.
[9] X. Zhang, X. Chen, C.L. Morfey, P.A. Nelson, Computation of spinning modal radiation from an unflanged duct, *8th AIAA/CEAS Aeroacoustics Conference*, Breckenridge, CO, 17–19 June 2002, AIAA Paper 2002-2475.
[10] X. Zhang, X. Chen, C.L. Morfey, P.A. Nelson, Acoustic radiation from a semi-infinite duct with a subsonic jet, *41st AIAA Aerospace Sciences Meeting*, Reno, NV, 6–9 January 2003, AIAA Paper 2003-0881.
[11] A.H. Nayfeh, D.P. Telionis, Acoustic propagation in ducts of varying cross sections, *Journal of the Acoustical Society of America* 54 (6) (1973) 1654–1661.
[12] S.W. Rienstra, Cut-on cut-off transition of sound in a slowly varying flow duct, in: L. Morino, N. Peake (Eds.), Aerotechnica, Missili e Spazio, special issue in memory of Prof. D.G. Crighton, 79, Nos. 3–4, 2000, p. 93–97.
[13] N.C. Ovenden, Near cut-on/cut-off transition in lined ducts with flow, *8th AIAA/CEAS Aeroacoustics Conference*, Breckenridge, CO, 17–19 June 2002, AIAA Paper 2002-2445.
[14] T. Elnady, H. Bodén, Hard strips in lined ducts, *8th AIAA/CEAS Aeroacoustics Conference*, Breckenridge, CO, 17–19 June 2002, AIAA paper 2002-2444.
[15] J. Yin, S. Ahmed, Helicopter main-rotor/tail-rotor interaction, *Journal of the American Helicopter Society* 45 (4) (2000) 293–302.
[16] M. Kuntz, Aeroacoustic Program System APSIM, User Handbook, Release 5.2, April, 2000.
[17] J. Yin, H. Buchholz, W. Splettstoesser, Numerical simulation of Bo105 main/tail rotor interaction noise and preliminary comparisons with flight test results, *28th European Rotorcraft Forum*, Bristol, England, 17–20 September, 2002.
[18] J.P. Berenger, A perfectly matched layer for the absorption of electromagnetic waves, *Journal of Computational Physics* 114 (1994) 185–200.
[19] R. Parker, Resonance effects in wake shedding from parallel plates: some experimental observations, *Journal of Sound and Vibration* 4 (1966) 62–72.
[20] W. Koch, Resonant acoustic frequencies of plate cascades, *Journal of Sound and Vibration* 88 (1983) 233–242.